Spontaneous formation of periodic nanostructured film by electrodeposition: Experimental observations and modeling

Yuan Wang,[1] Yu Cao,[1] Mu Wang,[1,2]* Sheng Zhong,[1] Ming-Zhe Zhang,[1] Yan Feng,[1] Ru-Wen Peng,[1] Xi-Ping Hao,[1] and Nai-Ben Ming[1]

[1]*National Laboratory of Solid State Microstructures and Department of Physics, Nanjing University, Nanjing 210093, China*

[2]*International Center for Quantum Structures, Chinese Academy of Sciences, Beijing 100080, China*

(Received 1 August 2003; published 27 February 2004)

In this paper we report the spontaneous formation of a nanostructured film by electrodeposition from an ultrathin electrolyte layer of $CuSO_4$. The film consists of straight periodic ditches and ridges, which corresponds to the alternating deposition of nanocrystallites of copper and copper plus cuprous oxide, respectively. The periodicity on the film may vary from 100 nm to a few hundred nanometers depending on the experimental conditions. In the formation of the periodically nanostructured film, oscillating voltage/current has been observed across the electrodes, and the frequency depends on the pH of the electrolyte and the applied current/voltage. A model based on the coupling of $[Cu^{2+}]$ and $[H^+]$ in the electrodeposition is proposed to describe the oscillatory phenomena in our system. The calculated results are in agreement with the experimental observations.

DOI: 10.1103/PhysRevE.69.021607 PACS number(s): 81.15.−z, 79.60.Jv, 81.16.Rf

I. INTRODUCTION

Oscillatory growth is frequently observed in electrochemical systems [1–8], and up to now much effort has been devoted to understanding the oscillations [9–22]. Generally an oscillation involves two or more competing factors, and the coupled equations associated with them may lead to oscillating solutions when certain requirements are satisfied. The oscillating concentration field of the chemical components in front of a growing interface may significantly affect the interfacial growth kinetics and the interfacial morphology. For example, it has been reported that the periodic change of concentration of the interfacial impurity may induce repeated transitions between dense-branching morphology and dendrites [23]. The concentration oscillation may also lead to periodic sidebranching [14,22] and alternating variations of the tip curvature in dendritic growth [15]. We recently observed a self-organized copper electrodeposition in an ultrathin layer of a $CuSO_4$ electrolyte, where periodic nanostructures were spontaneously generated on the deposit branches [24]. These periodic structures correspond to the alternating growth of copper and cuprous oxide. Instead of the spontaneous oscillation, people once applied an oscillating potential/current in electrodeposition, and composition-modulated multilayers of copper and cuprous oxide have been generated [21]. In previous film studies, however, much more attention has been paid to the formation of multilayered structures, i.e., the formation of periodic structures in the direction perpendicular to the substrate. The spontaneous formation of periodic nanostructures horizontally in the plane of the substrate has not been well studied. Nevertheless, this subject is of particular interest both for the understanding of the microscopic processes in electrodeposition, and for the fabrication of patterned nanostructures ''bottom-up'' by self-organization.

In this paper we demonstrate that the periodic nanostructures can be introduced horizontally on the film of Cu/Cu_2O electrodeposit by a self-organized growth. The periodicity can be tuned from 100 nm to a few hundred nanometers by changing the growth conditions. We find that the oscillation of electric current and the formation of the periodic nanostructures on the film are strongly correlated. Based on the experimental observations, a theoretical model is proposed to describe the oscillatory behavior. The calculated results are in good agreement with the experimental observations.

II. EXPERIMENTAL OBSERVATIONS

The electrodeposition was carried out in a cell made of two carefully cleaned glass plates. Two parallel, straight electrodes were 8.0 mm apart and fixed on the bottom glass plate [25,26]. The anode was made of pure copper wire (ϕ0.5 mm, 99.9% pure, Goodfellow, UK) and the cathode was a graphite bar 0.5 mm in diameter. The details of the experimental setup were reported in Refs. [24–26]. The electrolyte of $CuSO_4$ was confined in the space between the upper and lower glass plates and the electrodes. The electrolyte solution was prepared by analytical reagent $CuSO_4$ and deionized, ultrapure water (electric resistivity 18.2 MΩ cm). The initial concentration of the electrolyte was 0.05 M (pH $=4.5$). No special treatments (such as coating with metal clusters [27]) were made on the glass surface except conventional cleaning. A Peltier element was placed beneath the electrodeposition cell to modify the temperature. Both the deposition cell and the Peltier element were sealed in a thermostat chamber. Dry nitrogen gas flowed through the chamber to prevent water condensation on the glass window, so an *in situ* optical observation can be carried out. The temperature for electrodeposition was set below the freezing point of the original electrolyte, usually in the range between -0.2 to -5 °C for a 0.05-M $CuSO_4$ solution.

*Author to whom correspondence should be addressed. Email address: muwang@nju.edu.cn

To generate an ultrathin electrolyte layer for electrodeposition, a $CuSO_4$ solution was solidified by decreasing temperature [24–26]. To achieve a large, flat electrolyte-solid interface, great care was taken in the beginning of solidification to keep only one ice nucleus or just a few ice nuclei in the system. Several melting-solidification cycles were repeated to fulfill this requirement. In our system ice nucleus initiated on the bottom glass plate. During the solidification, $CuSO_4$ was partially expelled from the solid (this effect was known as partitioning effect [28,29] in crystallization). As a result, accompanying the solidification of the electrolyte, the concentration of $CuSO_4$ in front of the solid-electrolyte interface increased. Meanwhile, a very low solidification rate was used in order to prevent cellular growth [28,29]. On the other hand, it is known that the temperature at which the electrolyte solidifies (melting point/solidification point) depends on the concentration of the electrolyte. For $CuSO_4$ the solidification temperature decreases when the salt concentration is increased. Therefore, when the equilibrium was reached at a set temperature ($-4\,^{\circ}C$, for example), there still existed an ultrathin layer of concentrated $CuSO_4$ solution film between the ice of electrolyte (sosoloid of $CuSO_4$ and water) and the glass substrate. In our experiments electrodeposition was carried out in this ultrathin layer, where the $CuSO_4$ concentration was expected not to exceed the saturate concentration at the set temperature (at $-4\,^{\circ}C$ the saturate concentration of $CuSO_4$ was about 0.85 M). The thickness of this ultrathin layer depended on the initial electrolyte concentration and the setting temperature. At $-4\,^{\circ}C$ the thickness of this layer was around 200 nm (initial electrolyte concentration 0.05 M), which was estimated from the thickness of electrodeposit measured by atomic force microscopy. The electrodeposits were characterized with optical microscope (Leitz Orthoplan-pol), atomic force microscope (AFM) (Digital Instruments, Nanoscope IIIa) and field-emission scanning electron microscope (SEM) (LEO 1530VP), respectively.

Both galvanostatic and potentiostatic modes were used in the electrochemical deposition. No essential difference can be found on the morphology of the electrodeposits generated with these two modes. In the potentiostatic mode the applied constant voltage was in the range between 1.0 and 5.0 V, while in the galvanostatic mode the current was usually selected in the range of a few microampere up to 80 μA. The current/voltage across the electrodes during the electrodeposition was recorded as a function of time. Unlike the filaments normally observed at higher voltage (or stronger current) [24,25], here the electrodeposit forms a compact, solid film on the glass substrate with periodic line structures, as shown in Fig. 1(a). The film is not really flat. It contains periodically distributed ditches and ridges. The separation of the neighboring ditches (or ridges) is of the order of 500 nm when the experimental conditions are set as $V=1.5$, pH $=4.5$, and $T=-2.0\,^{\circ}C$. A detailed surface morphology of this structured film is shown in Fig. 1(b), where small grains in the thin film can be identified.

Figure 2 shows the very front edge of a film, from which one may understand how the film spreads over the glass substrate. Each ditch (ridge) on the film is in parallel with the

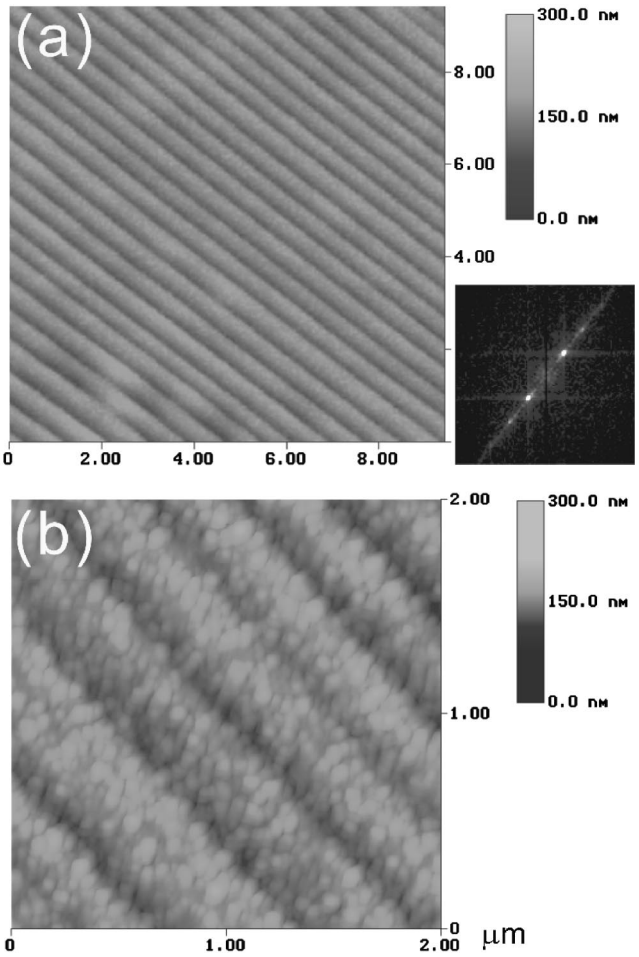

FIG. 1. (a) The compact, solid film deposited on the glass substrate viewed by AFM. Periodic structures can be identified on the film. The periodicity is about 500 nm. The inset is a two-dimensional Fourier transform of the picture, where the dominant spots represent the strict periodicity on the film. The experiment was carried out at $V=1.5$ V and $T=-2.0\,^{\circ}C$. The initial concentration of the electrolyte was 0.05 M. (b) The AFM view of the detail surface morphology of the structured film. It is clear that the film is made of small crystallites.

growth front, indicating that the ditches and the ridges are formed simultaneously when the film spreads over the substrate. The spatial periodicity shown in Fig. 2 is about 130 nm, and the experiment was carried out at $T=-3.5\,^{\circ}C$ and $I=5.5$ μA.

As we reported earlier, the formation of the periodic nanostructures on the electrodeposit is due to the spontaneous alternating growth of copper and cuprous oxide [24,25]. The fact that the crystallites of Cu_2O are concentrated in the ditches of the periodically structured film is confirmed by the scanning near-field optical microscopy (SNOM). The light source of the SNOM is an Ar ion laser, which generates three wavelengths: 465, 488, and 514 nm. Since the light of 514 nm can be strongly absorbed by Cu_2O, whereas it is not absorbed by copper, so we use this wavelength to do the experiments. Figure 3(a) shows the friction image of the structured film, where the periodicity can be clearly identified. Figure 3(b) shows the simultaneously measured absorp-

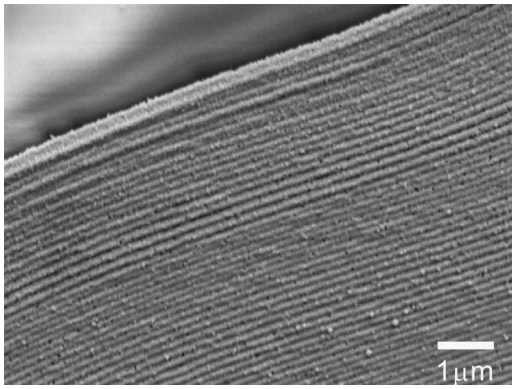

FIG. 2. The very front edge of the structured film viewed by scanning electron microscopy (SEM). The film develops horizontally over the insulating glass substrate: periodic ditches and ridges can be identified. The bright contrast on the upper-left corner is due to the electric charge accumulation in the insulating glass substrate in SEM observation. The periodicity on the film is of the order of 130 nm. The control parameters in the experiment are $I=5.5\ \mu$A and $T=-3.5\,^{\circ}$C and the initial concentration of the electrolyte was 0.05 M.

tion intensity over the same region as that shown in Fig. 3(a). The dark bands correspond to the strong absorption of Cu_2O. Although the resolution of Fig. 3 is not as high as that of Figs. 1 and 2, it can still be seen that the regions with strong absorption in Fig. 3(b) indeed correspond to the ditches in the morphology. This result is consistent with our previous studies of transmission electron microscopy [24,25].

During the formation of the periodic structures on the film, the voltage across the electrodes is oscillating (galvanostatic mode), as shown in Fig. 4(a). The Fourier transform of the oscillating voltage is illustrated in the inset, where the primary frequency is 0.2 Hz. The temporal oscillation of the electric signal and the spatial periodicity on the electrodeposits are precisely linked, which was demonstrated in our previous publications [24,25]. The oscillation relates to the applied current across the electrodes and pH of the electrolyte. As illustrated in Fig. 4(b), the measured fundamental oscillation frequency decreases when the solution becomes more acid. We find that if the electrolyte is sufficiently acid, no oscillations will be observed. The critical pH to ensure the oscillatory growth is 2.0 when the electric current is 40 μA, the electrolyte concentration is 0.05 M, and the temperature is $-2.0\,^{\circ}$C. We also observe that the fundamental oscillation frequency becomes higher when the electric current becomes stronger, as indicated in Fig. 4(c). The mechanism of the spontaneous oscillatory electrodeposition has indeed been discussed by several groups before [20,21,24], yet an analytical modeling seems not to be available. Since the directional growth of the thin film presented above can be regarded as one dimensional, in the following section we will try to establish a one-dimensional model to describe the oscillatory growth in our system.

III. MODELING THE CONCENTRATION OSCILLATION

Following the discussions in Ref. [30], the reactions in the copper electrodeposition can be written as

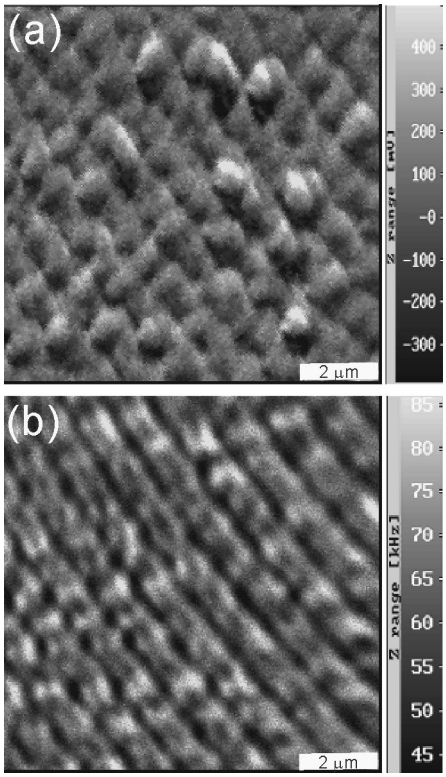

FIG. 3. The SNOM pictures of the structured film. (a) The friction image providing the morphological information of the film. (b) The simultaneous mapping of the absorption intensity over the same area of the film. Comparing (a) and (b) one may find that the strong absorption [dark strips in (b)] corresponds to the ditches in the morphology. The wavelength we used in the experiment (514 nm) is within the adsorbtion band of Cu_2O. We therefore conclude that the crystallites of cuprous oxide are much richer in the ditch regions than in the ridge regions. The experimental conditions for the sample preparation: $I=50\ \mu$A, $T=-0.3\,^{\circ}$C, pH=4.5, and $C=0.05$ M.

$$2Cu^{2+}+H_2O+2e^{-}\rightarrow Cu_2O\downarrow+2H^{+}, \tag{1}$$

$$Cu_2O+2H^{+}+2e^{-}\rightarrow 2Cu\downarrow+H_2O. \tag{2}$$

The reaction rates for Eqs. (1) and (2) are denoted as R_1 and R_2, respectively. The reaction rates can be expressed as

$$R_1=k_1\left[(C^0_{Cu^{2+}})^2-\frac{(C^0_{H^{+}})^2}{k}\right], \tag{3}$$

$$R_2=k_2(C^0_{H^{+}})^2, \tag{4}$$

where $C^0_{Cu^{2+}}$ and $C^0_{H^{+}}$ represent the interfacial concentration of Cu^{2+} and H^{+}, respectively, and k_1, k_2, and k are the kinetic coefficients for the reactions. Since the electrodeposition of copper is a far-from-equilibrium process, we may ignore the minus term in Eq. (3), i.e., the reverse reaction in Eq. (1) is neglected. So R_1 is simplified as

$$R_1=k_1(C^0_{Cu^{2+}})^2. \tag{5}$$

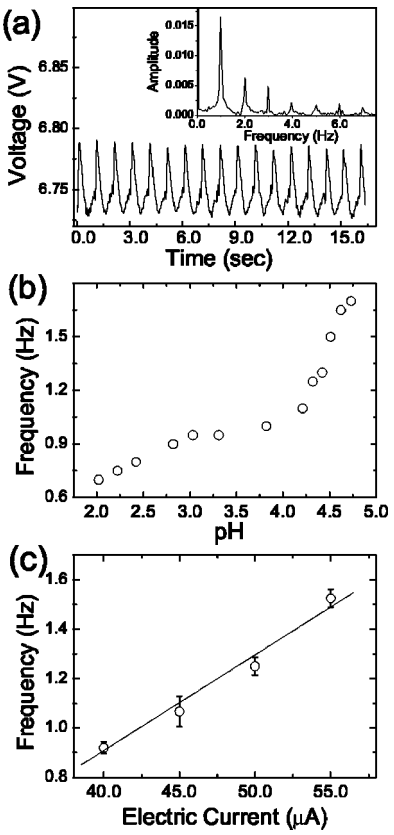

FIG. 4. (a) The oscillating voltage across the electrodes measured in the galvanostatic mode. The inset is the Fourier transform of the oscillating voltage. The experimental conditions are the following: $I=50\ \mu$A, $T=-2.0\,^{\circ}$C, pH=3.9, and $C=0.05$ M. (b) The dependence of the oscillation frequency as a function of the pH of the electrolyte. The experimental conditions are set as: $I=40\ \mu$A, $T=-4.7\,^{\circ}$C, and $C=0.05$ M. (c) The measured oscillation frequency as a function of the applied electric current. A linearly increasing relation can be found. The experimental conditions are set as: $T=-3.0\,^{\circ}$C, pH=4.5, and $C=0.05$ M.

Considering Eqs. (1) and (2) one may find that if $[H^+]$ is high, more Cu_2O will be changed to copper via reaction (2), which in turn will accelerate reaction (1). Therefore k_1 should increase monotonically when $[H^+]$ increases. We suggest that the coefficient k_1 is expressed as a polynomial format of the normalized concentration of H^+,

$$k_1=\alpha\left[1+\beta_1\frac{C^0_{H^+}}{C^\infty_{H^+}}+\beta_2\left(\frac{C^0_{H^+}}{C^\infty_{H^+}}\right)^2\right], \tag{6}$$

where $C^\infty_{H^+}$ and $C^0_{H^+}$ stand for $[H^+]$ far away from the growth front and at the growth front, respectively; α, β_1 and β_2 are positive constants. Since R_2 in Eq. (4) has already been proportional to the square of $[H^+]$, we take k_2 as a constant.

The concentration field and the electric field obey the following equations if convection is ignored in the ion transport:

$$\frac{\partial C_i}{\partial t}=D_i\nabla^2 C_i-\mu_i E\cdot\nabla C_i-\mu_i C_i\cdot\nabla E, \tag{7}$$

$$\nabla E=\frac{e}{\epsilon\epsilon_0}\sum_i z_i C_i, \tag{8}$$

where E is the electric field; C_i is the concentration field of species i, which covers all the cations and anions; D_i and μ_i are the corresponding diffusion coefficient and electric mobility, respectively. ϵ_0 is the vacuum permittivity; and ϵ is the dielectric constant of solution. $z_i e$ stands for the total charges of ion species i. For a sufficiently long rectangular cell, the boundary effect can be ignored. Hence Eqs. (7) and (8) are simplified as

$$\frac{\partial C_i}{\partial t}=D_i\frac{\partial^2 C_i}{\partial^2 x}-\mu_i\frac{\partial(C_i E)}{\partial x}, \tag{9}$$

$$\frac{\partial E}{\partial x}=\frac{e}{\epsilon\epsilon_0}\sum_i z_i C_i. \tag{10}$$

The space in front of the growing interface can be divided into three regions. One is a space-charge-region in the close vicinity of the cathode, where $C_c \gg C_a$ holds. The thickness of this charged region is δ. Outside of δ, away from the cathode there exists a quasineutral region ($\Sigma z_i C_i\approx 0$), which extends to the length L. Outside L the charge neutrality holds and both the concentration field of Cu^{2+} and H^+ are stable. Integrating both sides of Eq. (9) over L, and taking a linear approximation for both the quasineutral region and the space-charge region, we obtain

$$\frac{\delta}{2}\frac{\partial C^0_i}{\partial t}=D_i\left(\frac{\partial C_i}{\partial x}\right)^{x=L}_{x=0}-\mu_i E^L C^L_i+\mu_i E^0 C^0_i, \tag{11}$$

where E^L is defined as the strength of the electric field at boundary of electric neutrality ($x=L$), and can be determined from the experimental control parameters. Now we try to get the expression of the electric field at the growing interface, E^0. Since the electric field changes continuously in the solution, from Eq. (10) we have

$$E^0=E^L-\int_0^L\frac{e}{\epsilon\epsilon_0}\sum z_i C_i dx. \tag{12}$$

Note that the concentration of anions is negligible in the space-charge region; therefore $\Sigma z_i C_i=z_{Cu^{2+}}C_{Cu^{2+}}+z_{H^+}C_{H^+}$ for $x<\delta$. In the region $\delta<x<L$, $\Sigma z_i C^L_i\approx 0$ holds, and $\Sigma z_i C^L_i=0$ for $x>L$. So Eq. (12) is simplified as

$$E^0=E^L-\frac{e\delta}{\epsilon\epsilon_0}\left(C^0_{Cu^{2+}}+\frac{C^0_{H^+}}{2}\right). \tag{13}$$

On the other hand, the mass conservation at the deposit front ($x=0$) requires

$$D_i\left(\frac{\partial C_{Cu^{2+}}}{\partial x}\right)_{x=0} = R_1 = k_1 (C^0_{Cu^{2+}})^2; \tag{14}$$

$$D_i\left(\frac{\partial C_{H^+}}{\partial x}\right)_{x=0} = R_2 - R_1 = k_2 (C^0_{H^+})^2 - k_1 (C^0_{Cu^{2+}})^2. \tag{15}$$

For simplicity, we assume [31]

$$D_i\left(\frac{\partial C_i}{\partial x}\right)_{x=L} = D_i \frac{C^L_i}{L}. \tag{16}$$

By taking Eqs. (13)–(16) in Eq. (11), and defining the unified concentration field of Cu^{2+} and H^+ at the growth front as $u \equiv C^0_{Cu^{2+}}/C^L_{Cu^{2+}}$ and $v \equiv C^0_{H^+}/C^L_{H^+}$, respectively, we eventually get two coupled differential equations as

$$\frac{\partial u}{\partial t} = -\alpha' u^2 + \beta' u - \xi' uv + \gamma', \tag{17}$$

$$\frac{\partial v}{\partial t} = -\alpha v^2 + \theta u^2 + \beta v - \xi uv + \gamma, \tag{18}$$

where

$$\alpha' = \left(\frac{2k_1}{\delta} + \frac{\mu_{Cu^{2+}} e}{\epsilon\epsilon_0}\right) C^L_{Cu^{2+}},$$

$$\beta' = \frac{2\mu_{Cu^{2+}} E^L}{\delta},$$

$$\gamma' = \left(\frac{2D_{Cu^{2+}}}{\delta L} - \frac{2\mu_{Cu^{2+}} E^L}{\delta}\right),$$

$$\xi' = \frac{\mu_{Cu^{2+}} e C^L_{H^+}}{\epsilon\epsilon_0},$$

$$\alpha = \left(\frac{2k_2}{\delta} + \frac{\mu_{H^+} e}{\epsilon\epsilon_0}\right) C^L_{H^+},$$

$$\beta = \frac{2\mu_{H^+} E^L}{\delta},$$

$$\gamma = \left(\frac{2D_{H^+}}{\delta L} - \frac{2\mu^+_H E^L}{\delta}\right),$$

$$\theta = \frac{2k_1 (C^L_{Cu^{2+}})^2}{\delta C^L_{H^+}},$$

$$\xi = \frac{2\mu_{H^+} e C^L_{Cu^{2+}}}{\epsilon\epsilon_0}.$$

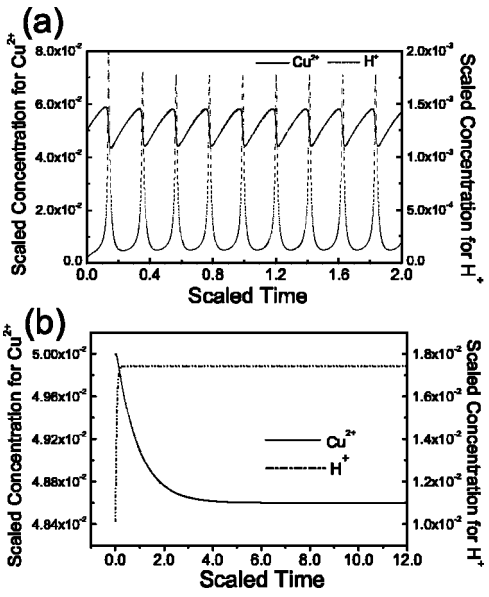

FIG. 5. According to the model described in the text, both concentrations $[Cu^{2+}]$ and $[H^+]$ may oscillate when the pH of the electrolyte is high. (a) shows the calculated oscillating $[Cu^{2+}]$ (the solid line) and $[H^+]$ (the dotted line), respectively. (b) If the pH of the electrolyte becomes sufficiently low, the concentration fields become stable and no oscillation can be identified.

IV. RESULTS AND DISCUSSION

By solving the coupled nonlinear differential equations (17) and (18) numerically, we can get the dynamic behavior of both $[Cu^{2+}]$ and $[H^+]$ in front of the growing interface. We find that both the concentrations are oscillating when pH of the solution is set to a proper value. Figure 5(a) shows the oscillating $[Cu^{2+}]$ and $[H^+]$ as a function of time. The oscillation of $[Cu^{2+}]$ takes place simultaneously with the oscillation of $[H^+]$. When the pH of the electrolyte becomes sufficiently low, however, the oscillatory behavior disappears. Figure 5(b) shows the dynamic behavior of the concentrations when the pH is as low as 2.0. Meanwhile the concentrations have been completely stabilized.

The numerical calculation also shows that the oscillation frequency depends on both the pH of the electrolyte and the applied voltage across the electrodes. Figure 6(a) illustrates that the oscillation frequency increases monotonically as a function of the pH, which is consistent with the experimental observations [Fig. 4(b)]. The electric field far away from the electrode, E^L, is determined by the separation of the electrodes and the voltage across the electrodes, which can be experimentally tuned. We calculate the frequency of the concentration oscillation as a function of the electric field E^L, as shown in Fig. 6(b). The temporal oscillation frequency increases when the electric field becomes stronger. This result is in agreement with the experimental observation shown in Fig. 4(c), where the measured frequency increases when the electric current becomes stronger.

From the definitions of R_1 and R_2 one may find that R_1 and R_2 depend nonlinearly on the oscillating concentrations of Cu^{2+} and H^+. By studying the evolution of R_1 and R_2, we may get a clearer picture of the alternating deposition of

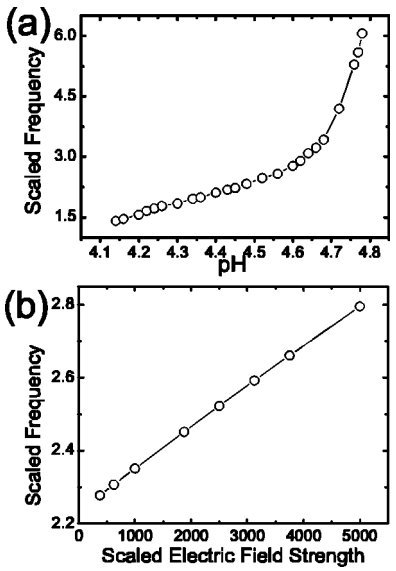

FIG. 6. (a) The calculated oscillation frequency as a function of the pH of the electrolyte solution. The tendency of this curve is consistent with the experimental observation [Fig. 4(b)]. (b) The calculated oscillation frequency as a function of the electric field. This result is in agreement with that shown in Fig. 4(c).

copper and cuprous oxide. Figure 7 illustrates the reaction rates R_1 and R_2 as a function of $[H^+]$. Corresponding to the oscillation of $[H^+]$, R_1 evolutes clockwise following the route *A-B-C-D-E-F-A*, whereas R_2 oscillates along the route *A-G-D-G-A*. When R_1 evolute from *A* to *B*, *C*, and *D*, R_2 evolute from *A-G-D*. In this process, $R_1 \geqslant R_2$, and both Cu_2O and Cu are generated. Meanwhile $[H^+]$ increases gradually. At point *D*, $R_1 = R_2$, meaning that all the Cu_2O generated in reaction (1) becomes copper via the reaction (2), and no extra Cu_2O remains. Thereafter, as R_1 develops along *D-E-F-A*, and R_2 develops from *D-G-A*, $R_1 \leqslant R_2$. During this period, only Cu is generated, and $[H^+]$ is gradually consumed. By repeating these processes, copper and cuprous oxide generate alternatingly and the periodic structures as those shown in Figs. 1–3 are achieved. Therefore, the coupling and interaction between reactions (1) and (2) lead to the alternating deposition of copper and cuprous oxide.

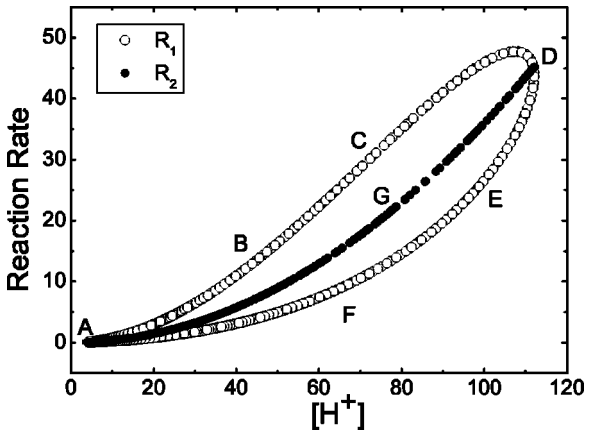

FIG. 7. The reaction rates R_1 and R_2 plotted as a function of $[H^+]$. R_1 develops clockwise in a loop, whereas R_2 oscillates along the line *A-G-D*.

Although quite a few simplifications are used in our calculation, this model still describes the essential processes in front of the growing interface when the electrolyte concentration is not too high. As we mentioned in Sec. II, a sufficiently high pH of the electrolyte is required in order to observe the oscillatory growth in experiments. In the calculation, our model shows that if the pH value of the electrolyte is set very low, the concentration fields in front of the deposit will be stabilized. Meanwhile, R_2 is always higher than R_1, and all the Cu_2O generated in Eq. (1) changes to copper. As a result, no periodic structures can be generated on the deposit. This may explain the fact that in the electrochemical coating of copper, very often acidic environment is used.

The thin film electrodeposition reported here differs from previous ones in following ways. First, in previous studies of thin film growth, people mostly focus on how a film develops in the direction perpendicular to the substrate. In our system, however, we are more interested in the horizontal propagation of the film over a substrate. It should be noted that the substrate itself in our experiments is not electrically conductive. The electrodeposition takes place via the successive nucleation at the concave corner of the electrodeposit and the substrate. This deposition process, to the best of our knowledge, has not been well studied before. Second, here we demonstrate a one-dimensional analog to the two-dimensional layered film growth. In other words, in our case the film develops ''line by line'' horizontally over the substrate instead of growing ''layer by layer'' in the direction perpendicular to the substrate. The observations reported here actually raise a few questions to the fundamentals of interfacial growth. For example, the thin film growth presented here is essentially a nucleation-limited polycrystalline aggregation, whereas the line by line growth behaviors make us think about why and how these lines keep straight and stable. It seems that there should exist an equivalent interfacial tension in the polycrystalline aggregation, which keeps the aggregation front smooth.

In addition, we are also interested in the stability of the concentration fields and the corresponding interfacial morphologies. As a matter of fact, what we demonstrate in this paper is that the concentration in front of the aggregate changes with time, but along the aggregate front the concentration is homogeneous and constant. This scenario can be more clearly seen by sitting on a moving coordinate system fixed on the aggregate front. Meanwhile the temporal oscillation of the concentration in the moving coordinate system results in the spatial periodicity on the electrodeposit (Figs. 1–3). What will happen if instability occurs to the concentration field along the growth front? Recently we indeed observed such an example, where additional periodicity has been introduced along the growth front, so a two-dimensional periodic pattern can be spontaneously formed. Details will be reported separately [32].

As we stated earlier, the periodic structures (ditches and ridges) on the electrodeposits correspond to the alternating growth of copper and copper plus cuprous oxide. Meanwhile

the film becomes anisotropic along the growth direction and perpendicular to the growth direction. We suggest that the electric properties of such a film should be anisotropic as well: those ''lines'' corresponding to the copper crystallites are metallic, while the neighboring Cu_2O-rich ''lines'' are electrically more semiconductive. This structured film might have some interesting physical features. The alternating and direct electric properties of such a structured film are now under investigation.

To summarize, we report in this article the spontaneous formation of a periodically nanostructured film by electrodeposition. The periodic structure corresponds to the alternating deposition of nanocrystallites of copper and cuprous oxide, which has been experimentally confirmed. Oscillating current/voltage has been measured during the formation of the structured film. The dependence of the temporal oscillation on the pH of the electrolyte and the applied electric current across the electrodes has been investigated. A model is proposed to describe the oscillatory growth in our system. The calculated results are qualitatively in agreement with the experimental observations.

ACKNOWLEDGMENTS

This work was supported by projects from the National Natural Science Foundation of China (10021001 and 10374043) and from the Ministry of Science and Technology of China (G1998061410).

[1] J. Wotjowicz, in *Modern Aspects of Electrochemistry*, edited by J. O. M. Bockris and B. E. Conway (Plenum, New York, 1972), Vol. 8, p. 47.
[2] J. Wotjowicz, N. Maeincic, and B.E. Conway, J. Chem. Phys. **48**, 4333 (1968).
[3] H. Moreira and R. de Levie, J. Electroanal. Chem. **29**, 353 (1971).
[4] J.F. Cooper, R.H. Muller, and C.W. Tobias, J. Electrochem. Soc. **132**, 1031 (1980).
[5] M.R. Basset and J.L. Hudson, Chem. Eng. Commun. **60**, 145 (1987).
[6] F.N. Albahadily and M. Shell, J. Chem. Phys. **88**, 4312 (1988).
[7] H.P. Lee, K. Nobe, and A. Pearlstein, J. Electroanal. Chem. **132**, 1031 (1985).
[8] F. Argoul and A. Kuhn, J. Electroanal. Chem. **359**, 81 (1993).
[9] C. Cachet, B. Saidani, and R. Wiart, J. Electrochem. Soc. **139**, 645 (1992).
[10] R.M. Suter and P.Z. Wong, Phys. Rev. B **39**, 4536 (1989).
[11] F. Argoul and A. Arneodo, J. Phys. (France) **51**, 2477 (1990).
[12] F. Argoul, J. Huth, P. Merzeau, and A. Arneodo, Physica D **62**, 170 (1993).
[13] J. St. Pierre *et al.*, Electrochim. Acta **25**, 827 (1980).
[14] M. Wang and N.B. Ming, Phys. Rev. A **45**, 2493 (1992).
[15] M. Wang, N.B. Ming, and P. Bennema, Phys. Rev. E **48**, 3825 (1993).
[16] D. Piron, I. Nagatsugawa, and C. Fan, J. Electrochem. Soc. **138**, 3296 (1991).
[17] F.W. Schlitter, G. Eichkorn, and H. Fischer, Electrochim. Acta **13**, 2063 (1968).
[18] H.D. Dorfler and E. Muller, J. Electroanal. Chem. **135**, 37 (1982).
[19] J.A. Switzer and T.D. Golden, Adv. Mater. (Weinheim, Ger.) **5**, 474 (1993).
[20] J.A. Switzer, C.-J. Hung, L.-Y. Huang, E.R. Switzer, D.R. Kammler, T.D. Golden, and E.W. Bohannan, J. Am. Chem. Soc. **120**, 3530 (1998).
[21] E.W. Bohannan, L.Y. Huang, F.S. Miller, M.G. Shumsky, and J.A. Switzer, Langmuir **15**, 813 (1999).
[22] S. Wang, K.Q. Zhang, Q.Y. Xu, M. Wang, R.W. Peng, Z. Zhang, and N.B. Ming, J. Phys. Soc. Jpn. **72**, 1574 (2003).
[23] M. Wang and N.B. Ming, Phys. Rev. Lett. **71**, 113 (1993).
[24] M. Wang, S. Zhong, X.B. Yin, J.M. Zhu, R.W. Peng, Y. Wang, K.Q. Zhang, and N.B. Ming, Phys. Rev. Lett. **86**, 3827 (2001).
[25] S. Zhong, Y. Wang, M. Wang, M.Z. Zhang, X.B. Yin, R.W. Peng, and N.B. Ming, Phys. Rev. E **67**, 061601 (2003).
[26] S. Zhong, M. Wang, X.B. Yin, J.M. Zhu, R.-W. Peng, Y. Wang, and N.B. Ming, J. Phys. Soc. Jpn. **70**, 1452 (2001).
[27] V. Fleury and D. Barkey, Europhys. Lett. **36**, 253 (1996).
[28] N.-B. Ming, *Fundamentals of Crystal Growth Physics* (Shanghai Science and Technology, Shanghai, 1982).
[29] A. Pimpinelli and J. Villain, *Physics of Crystal Growth* (Cambridge University Press, Cambridge, 1998).
[30] Y.C. Zhou and J.A. Switzer, Scr. Mater. **38**, 1731 (1998).
[31] Here we actually assume $C_i^o = 0$, and a linear approximation is used, so the concentration gradient at $x = L$ equals C_i^L/L.
[32] M. Wang (unpublished).